Monthly Notices of the ROYAL ASTRONOMICAL SOCIETY LETTERS

Mon. Not. R. Astron. Soc. **424,** L11–L15 (2012) doi:10.1111/j.1745-3933.2012.01275.x

# RAMSES-CH: a new chemodynamical code for cosmological simulations

C. G. Few,[1⋆] S. Courty,[2] B. K. Gibson,[1,3,4] D. Kawata,[5] F. Calura[1,6] and R. Teyssier[7,8]

[1]*Jeremiah Horrocks Institute, University of Central Lancashire, Preston PR1 2HE*
[2]*Université de Lyon; Université Lyon 1, Observatoire de Lyon, 9 avenue Charles André, Saint-Genis Laval F-69230, France; CNRS, UMR 5574, Centre de Recherche Astrophysique de Lyon; Ecole Normale Supérieure de Lyon*
[3]*Monash Centre for Astrophysics, School of Mathematical Sciences, Monash University, Clayton, VIC 3800, Australia*
[4]*Department of Astronomy & Physics, Saint Mary's University, Halifax, NS B3H 3C3, Canada*
[5]*Mullard Space Science Laboratory, University College London, Holmbury St Mary, Dorking, Surrey RH5 6NT*
[6]*Instituto Nazional di Astrofisica, Osservatorio Astronomico di Bologna, Via Ranzani 1, I-40127 Bologna, Italy*
[7]*Institute for Theoretical Physics, University of Zürich, CH-8057 Zürich, Switzerland*
[8]*UMR AIM, CEA Saclay, 91191 Gif-sur-Yvette, France*

Accepted 2012 April 21. Received 2012 April 19; in original form 2012 February 23

## ABSTRACT

We present a new chemodynamical code – RAMSES-CH – for use in simulating the self-consistent evolution of chemical and hydrodynamical properties of galaxies within a fully cosmological framework. We build upon the adaptive mesh refinement code RAMSES, which includes a treatment of self-gravity, hydrodynamics, star formation, radiative cooling and supernova feedback, to trace the dominant isotopes of C, N, O, Ne, Mg, Si and Fe. We include the contribution of Type Ia and Type II supernovae, in addition to low- and intermediate-mass asymptotic giant branch stars, relaxing the instantaneous recycling approximation. The new chemical evolution modules are highly flexible and portable, lending themselves to ready exploration of variations in the underpinning stellar and nuclear physics. We apply RAMSES-CH to the cosmological simulation of a typical $L_\star$ galaxy, demonstrating the successful recovery of the basic empirical constraints regarding [α/Fe]–[Fe/H] and Type Ia/II supernova rates.

**Key words:** galaxies: evolution – galaxies: formation – methods: numerical.

## 1 INTRODUCTION

The determination of elemental abundance patterns is one of the primary diagnostics of galaxy formation, with numerous spatial and temporal trends between age, kinematics and chemistry guiding our insights into the underpinning physical processes. Observations of abundance ratios corroborate our understanding of the nuclear physics governing $\alpha$-element production in that they are produced on shorter time-scales than iron-peak elements (e.g. Carbon et al. 1987; Edvardsson et al. 1993; Reddy, Lambert & Allende Prieto 2006; Ramírez, Allende Prieto & Lambert 2007), as a consequence of the mass-dependent nuclear burning processes acting within the relevant progenitor stars. Galactic chemical evolution (CE) models are predicated upon a coupling of these elemental production sites/time-scales with phenomenological (yet, empirically constrained) parametrizations of star formation and gas inflows/outflows. The resulting predicted abundance patterns can be compared directly with observations in order to shed light on the formation and evolution of the system under study.

The formalism associated with the seminumerical approach to galactic CE (e.g. Talbot & Arnett 1971; Pagel & Patchett 1975; Tinsley 1980; Matteucci & Francois 1989; Carigi 1994; Chiappini, Matteucci & Gratton 1997; Gibson 1997; Ramírez et al. 2007) is a powerful tool when applied to subgrid CE treatments within fully hydrodynamical simulations. The inclusion of CE schemes has been achieved in a number of cosmological hydrodynamical codes (e.g. Lia, Portinari & Carraro 2002; Kawata & Gibson 2003; Valdarnini 2003; Kobayashi 2004; Tornatore et al. 2004; Romeo, Portinari & Sommer-Larsen 2005; Martínez-Serrano, Domínguez-Tenreiro & Mollá 2008; Oppenheimer & Davé 2008; Wiersma et al. 2009; Shen, Wadsley & Stinson 2010), each of which is based upon smoothed particle hydrodynamics (SPH). Key lessons can be learned from an examination of the role that CE plays in the physics of the interstellar medium (ISM). This is manifest in the metallicity-dependent radiative cooling rates of plasmas and their impact on the efficiency of metal transport throughout the disc and its consequent impact on stellar chemodynamics (Scannapieco et al. 2005). This impact upon turbulence-driven metal transport can be problematic, in the light of known issues concerning the ability of conventional treatments of SPH to resolve the associated instabilities in certain regimes; such problems are ameliorated (though not entirely) by Eulerian approaches to fluid dynamics, including adaptive mesh

⋆E-mail: c.gareth.few@googlemail.com

© 2012 The Authors
Monthly Notices of the Royal Astronomical Society © 2012 RAS

Downloaded from http://mnrasl.oxfordjournals.org/ at Saint Mary's University on November 5, 2014

refinement (AMR) schemes (e.g. O'Shea et al. 2005; Agertz et al. 2007; Tasker et al. 2008).

In its simplest form, interparticle 'mixing' of SPH particles does not occur, i.e. metal-rich and metal-poor gas particles may coexist near each other without sharing/mixing their associated metals. The impact of this lack of mixing is readily apparent in a galaxy simulation's metallicity distribution function and age–metallicity relation, as well as the abundance ratio plane (e.g. Pilkington, Gibson & Jones 2012). The inclusion of turbulent mixing models within SPH remedies this lack of implicit diffusion (Shen et al. 2010), even if the associated diffusion coefficient is a necessary additional free parameter (albeit informed by turbulence theory).

With the intention of providing a complementary (AMR) approach to extant (SPH) chemodynamical and seminumerical CE models, we present what is, to our knowledge, the first cosmological AMR code which implements a temporally resolved feedback and CE prescription. Written as a patch to the gravitational cosmological *N*-body and hydrodynamical code RAMSES, we now include the effects of Type II supernovae (SNeII), Type Ia supernovae (SNeIa) and low-mass to intermediate-mass asymptotic giant branch (AGB) stars, both from an energetic and chemical perspective. Nucleosynthetic processes are accounted for as a function of progenitor mass and metallicity. The CE module is described in Section 2. The mechanics of marrying of this module to the AMR code RAMSES, leading to the self-consistent chemodynamical code RAMSES-CH, is outlined in Section 3. Finally, in Section 4, we present a demonstration of the ability of the code to reproduce basic observational constraints. We emphasize that this Letter is primarily a methodological description for coupling CE with AMR, and that future papers in this series will explore the response of RAMSES-CH to the various input parameters and assembly histories.

## 2 CHEMICAL EVOLUTION MODEL

The underlying CE model used to determine the relative rates of SNeII; SNeIa and AGB, and the associated chemical enrichment, for a stellar population governed by a given initial mass function (IMF), is generated prior to the simulation being run. The resulting look-up tables provide the SNII, SNIa and isotopic return rates as a function of time for a range of simple stellar population (SSP) metallicities. The code (provided as part of the RAMSES-CH patch) is flexible, allowing the user to readily modify relevant stellar physics via the importation of different SN and AGB yields, as well as the IMF.

For this first work, we have adopted a fairly standard/conservative CE model, employing a Kroupa (2001) IMF with stellar mass limits of 0.1 and 100 $M_\odot$. We also used a SNIa delayed time distribution formalism similar to that presented in Kobayashi, Tsujimoto & Nomoto (2000) and Kawata & Gibson (2003), with the simplification that the IMF slope for both the primaries and secondaries was taken to be identical. Stellar lifetimes were taken from Kodama & Arimoto (1997) and are dependent upon both mass and metallicity. The yields of SNII progenitors (11–40 $M_\odot$), for metallicities spanning Population III to solar, are from Woosley & Weaver (1995); for $m > 30\,M_\odot$, we adopt the yields associated with the Model B explosion energies, after Timmes, Woosley & Weaver (1995) and Kawata & Gibson (2003). Massive stars in the range 8–40 $M_\odot$ are assumed to explode as SNeII, where the yields in the range 8–11 $M_\odot$ are found by scaling the elemental mass fractions of the 11 $M_\odot$ stars with the progenitor mass. The same process is used to calculate the yields of stars down to 0.1 $M_\odot$ using the lowest mass (0.8 $M_\odot$)

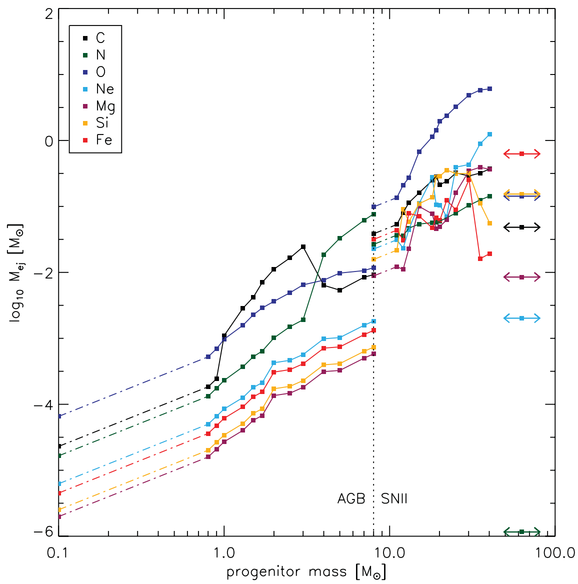


**Figure 1.** Mass of elements ejected by stars as a function of initial mass. Also shown are the abundances for a single SNIa (horizontal arrows) for comparison (the position along the abscissa is arbitrary, chosen to avoid conflict with other data). The mass above which stars are considered to be SNII progenitors is indicated at 8 $M_\odot$. Data for AGB stars are taken from van den Hoek & Groenewegen (1997), SNeII from Woosley & Weaver (1995) and SNeIa from Iwamoto et al. (1999). Points connected by solid lines denote the original data, while those connected by dot–dashed lines show adopted extrapolations to lower masses. Extrapolations are linear and scaled to the mass of the progenitor star.

AGB star available in van den Hoek & Groenewegen (1997). The yields adopted are illustrated in Fig. 1.

As noted earlier, nucleosynthetic yields for SNeIa were taken from Iwamoto et al. (1999). In addition to the time constraints imposed by the mass range of the secondaries in the SNIa (binary) progenitors, Hachisu, Kato & Nomoto (1999) also suggest the use of a metallicity 'floor' which suppresses the formation of low-metallicity ([Fe/H] $< -1.1$) SNIa progenitors. In the light of the ongoing controversy regarding this putative metallicity floor, we have adopted the conventional assumption that low-metallicity binaries are capable of forming SNIa progenitors. These SNIa yields are also noted in Fig. 1 by the horizontal arrows.

The time evolution of the isotopic ejection rate (per unit mass) from an SSP is shown in Fig. 2. The RAMSES-CH CE model generates a family of such ejection rates for any combination of yield compilation and IMF. We have chosen to simply show the impact of the choice of one conservative combination of parameters. This should not be construed as implying that this combination is necessarily the best or unique pairing; it is simply chosen to demonstrate the efficacy of the methodology.

### 3 RAMSES-CH

We have introduced the CE prescription into the v3.07 public release version of RAMSES (Teyssier 2002). Prior to these enhancements, RAMSES tracked the total gas metallicity (*Z*), under the assumption of the instantaneous recycling approximation and treating *Z* as a passive scalar advected by the hydrodynamical flow. Our new chemodynamical version (RAMSES-CH) also employs passive scalars in the tracking of the dominant isotopes of H, C, N, O, Mg, Ne, Si and Fe, and the chemical composition of the gas from which the stellar particles form is 'tagged' on to the new particles. As

© 2012 The Authors, MNRAS **424,** L11–L15
Monthly Notices of the Royal Astronomical Society © 2012 RAS

Downloaded from http://mnrasl.oxfordjournals.org/ at Saint Mary's University on November 5, 2014

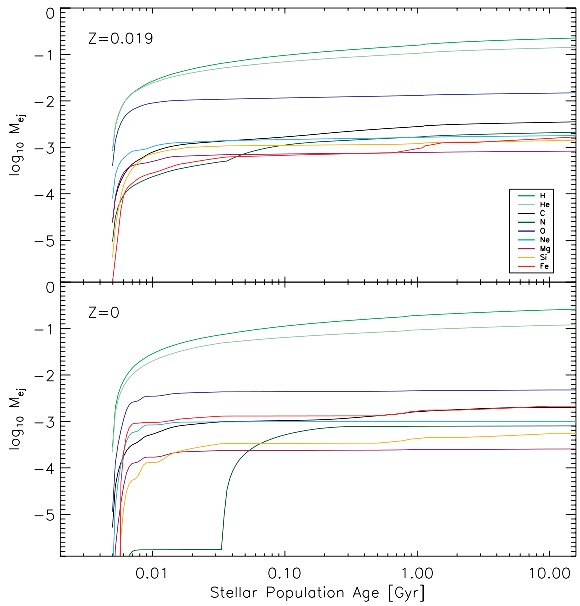


**Figure 2.** Ejection rate of dominant elemental isotopes, per unit stellar mass, as a function of age for a Kroupa (2001) IMF. The upper and lower panels correspond to solar and Population III metallicity SSPs, respectively.

described by Dubois & Teyssier (2008), star particles are created in the high-density gas ($\rho_{\rm gas} > \rho_{\rm th}$) and spawned by a random Poisson process following a rate given by $\dot{\rho}_* = \epsilon_* \rho_{\rm gas}/t_{\rm ff}$, where $t_{\rm ff}$ is the local free-fall time of the gas, $(3\pi/32G\rho_{\rm gas})^{1/2}$, and $\epsilon_*$ is the star formation efficiency. Each stellar particle enriches the surrounding ISM according to its individual chemical history recorded in the look-up tables described in Section 2, depending upon the particle's initial mass and metallicity. Chemical enrichment and feedback processes are treated simultaneously through a kinetic feedback mode. While we could apply kinetic feedback to all the stellar populations, we do so only to those stellar populations that include SNII events. A thermal feedback mode is used when the stellar population ages and enters an AGB 'phase' and a SNIa 'phase'. The kinetic feedback mode aims at reproducing those expanding gas flows generated by the collective explosions of massive stars. At each time-step, density, momentum, energy and metals are deposited into all gas cells situated within a feedback 'sphere' of a user-specified radius centred upon the young star particles. We set up our SNII feedback sphere radius to two grid cels. The velocity of the entrained gas, linearly interpolated with the radius, is given by the number of SNII events, the energy generated by each event $\epsilon_{\rm SN} E_{\rm SN}$ ($\epsilon_{\rm SN}$ being the efficiency with which the energy $E_{\rm SN} = 10^{51}$ erg couples to the surrounding ISM) and the total amount of gas to be entrained by the bubble. The entrained gas includes the gas released/ejected during the SNII events as well as the gas swept up by the bubble (Dubois & Devriendt, private communication). This latter component is parametrized as $f_w$ times the ejected gas mass ($f_w = 10$ in this work, corresponding to a mass loading factor of $\eta_w = 1$ for a standard run with a massive star fraction of 10 per cent). The galactic outflow scheme just described is not applied for the SNIa events, and when the stellar population enters an AGB and/or SNIa phase, feedback processes and chemical enrichment are handled 'locally' (thermally) and confined to the gas cell within which the stellar particle sits. The feedback algorithm is simplified by this approximation; future developments of the code will include kinetic SNIa feedback.

This new chemodynamical version of RAMSES was then applied in the generation of a multiresolved, cosmological simulation of a late-type disc galaxy (hereafter `109-CH`) with a virial mass of $7.1 \times 10^{11}$ M$_\odot$, whose initial conditions match those outlined in an earlier study (Sánchez-Blázquez et al. 2009). To remind the reader, the box size for this run was $L = 20\,h^{-1}$ Mpc, with a dark matter particle mass of $6 \times 10^6$ M$_\odot$ in the most refined region. The spatial resolution, kept roughly constant in physical size during the simulation, reaches $L/2^{\rm lmax} = 436$ pc at $z = 0$, with lmax $= 16$ levels of refinement. For this resolution, we choose a star formation density threshold $\rho_{\rm th}$ corresponding to $0.3\,{\rm cm}^{-3}$ and an efficiency of 1 per cent. The same SN energy coupling efficiency of $\epsilon_{\rm SN} = 1$ is assumed for both SNeII and SNeIa. A polytropic equation of state $T = T_{\rm th}(\rho/\rho_{\rm th})^{\gamma-1}$ is used in the high-density areas with a temperature threshold of 2900 K and a polytropic index $\gamma = 2$, allowing the Jeans length to be resolved by more than four cells at all times. Note that our feedback parameter choices are suitable for the implementation described here at resolutions of 100–500 pc.

## 4 CHEMODYNAMICS OF AN $L_\star$ GALAXY

We introduce this new grid-based chemodynamical tool to the community. We now demonstrate the efficacy of RAMSES-CH through a presentation of the chemical properties of `109-CH`. Future papers in this series will extend beyond this initial demonstration into a comprehensive chemical tagging and chemodynamical exploration of a suite of higher resolution cosmological discs spanning a range of environments and assembly histories, realizations of which are described in Pilkington et al. (2012).

The first metric to consider when introducing SNeII and SNeIa in parallel with a relaxation of the instantaneous recycling approximation is the predicted SN rates and a comparison with empirical constraints. We show the time evolution of these rates in Fig. 3. For `109-CH`, a present-day SNIa rate of 0.131 SNuM (SNe per

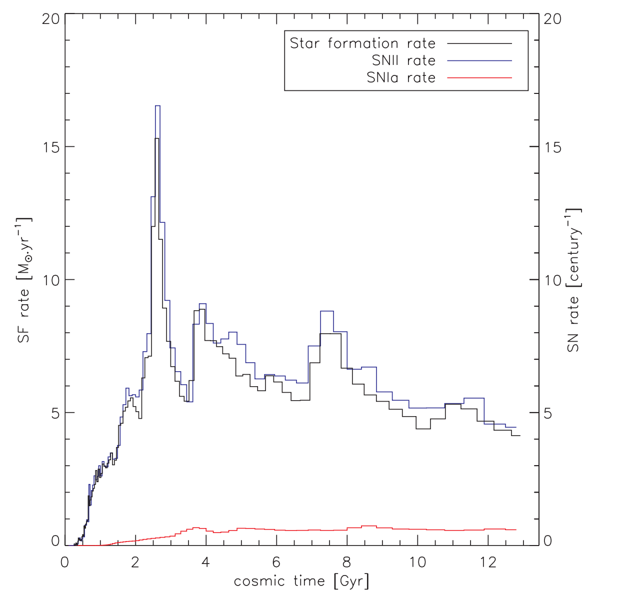


**Figure 3.** The star formation rate for `109-CH` is shown in black (refer to the left-hand ordinate) and the corresponding SNII and SNIa rates are shown (refer to the right-hand ordinate) in blue and red, respectively. Note that the SNII rate is not precisely proportional to the star formation rate as would be the case for data simulated using the 'standard' version of RAMSES. The SNII rate at each time is now dependent on the star formation rate of past as well as present time-steps.

© 2012 The Authors, MNRAS **424,** L11–L15
Monthly Notices of the Royal Astronomical Society © 2012 RAS

Downloaded from http://mnras.oxfordjournals.org/ at Saint Mary's University on November 5, 2014

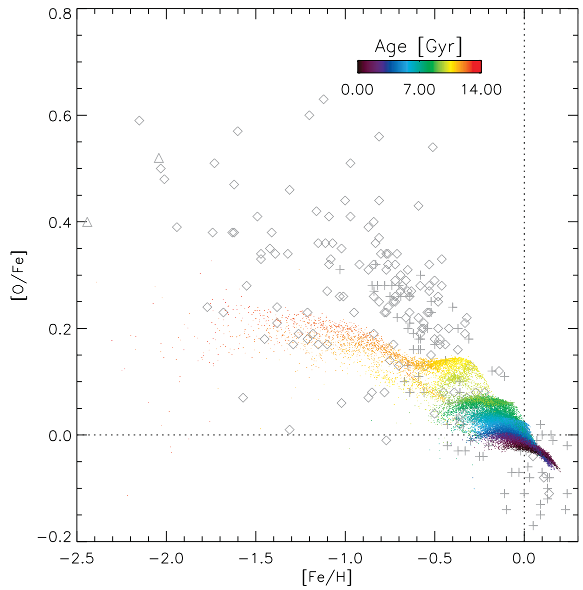


**Figure 4.** Abundance ratios of stars in a disc region of galactocentric radius between 5 and 11 kpc and within 3 kpc of the disc plane. Particles are coloured according to their age. Observational data are plotted in grey; triangles are very metal poor stars from Cayrel et al. (2004), diamonds are thick disc and halo stars from Gratton et al. (2003) and plus symbols are disc dwarf stars from Edvardsson et al. (1993). All data have been normalized to the solar abundance determination of Anders & Grevesse (1989).

century per $10^{10}\,M_\odot$ stellar mass) was found, and a SNII rate of 0.959 SNuM. Both the absolute values and SNeII:SNeIa ratio ($\sim$7) are consistent with those found by Mannucci et al. (2008) for field Sbc/d galaxies: $0.140^{+0.045}_{-0.035}$ SNuM for SNeIa and $0.652^{+0.164}_{-0.134}$ SNuM for SNeII.

Moving beyond the SN rates, the abundance ratios of readily observed elements are regularly employed to constrain the time-scales of star formation and therefore both feedback and fundamental nucleosynthesis. The recovery of empirical trends found locally in the solar neighbourhood is a necessity for any CE model. Such observations demonstrate a clear correlation between $\alpha$-element and iron abundances, in the sense of their being an $\alpha$-enhanced plateau at lower metallicities (below, say, [Fe/H] $\sim -0.7$) with a systematic decline to solar values, at higher metallicities (e.g. Edvardsson et al. 1993; Gratton et al. 2003; Reddy et al. 2003, 2006; Cayrel et al. 2004; Bensby et al. 2005). This empirical behaviour in [$\alpha$/Fe]–[Fe/H] can be seen in Fig. 4, where, in this case, we are showing the observational trends for [O/Fe] versus [Fe/H]. Also shown in Fig. 4 is the same distribution of [O/Fe]–[Fe/H] for the star particles at redshift $z = 0$ within an analogous ‘solar neighbourhood’ for the simulated disc `109-CH`. We should emphasize that the solar normalization employed for both simulated and observed data is that of Anders & Grevesse (1989).

A rigorous analysis of how the choice of SNII, SNIa and AGB yields, in addition to the IMF and SNIa progenitor model, impacts upon the chemodynamical evolution is left to future papers in this series, but it should be clear that even with this first ‘test’, the qualitative chemical properties are not inconsistent with observations of the local plateau+decline behaviour seen in the [$\alpha$/Fe]–[Fe/H] plane. Abundance ratios are recovered and the qualitative behaviour of the [Fe/H] $\sim -0.7$ knee is also seen in the simulated data. The knee feature seen in Fig. 4 at [O/Fe] = 0.15 and [Fe/H] = $-0.2$ is attributed to the bursty star formation profile which naturally creates multiple knee features as the SNII and SNIa rate fluctuates.

Examination of the age distribution (represented by the colour coding shown in the inset to Fig. 4) reveals rapid early enrichment in [Fe/H], similar to the age–metallicity relations predicted by classical CE models. Specifically, it takes $\sim$3 Gyr to reach a metallicity [Fe/H] $\approx -0.4$, driven by the initial phases of intense star formation, after which the age–metallicity relation flattens and the rate of growth of [Fe/H] consequently slows (even while SNeIa are becoming more important). This phase is characterized by the abundance ratio ‘strata’ seen in Fig. 4, with discrete ‘arcs’ appearing at decreasing values of [O/Fe] as time progresses.

The influence of the cosmological environment of this simulation is apparent in the abundance patterns of the galaxy. The subsample displayed in Fig. 4 exhibits the signature of merger events, e.g. the feature at [O/Fe] = 0.15 and [Fe/H] = $-0.2$. The full extent of this is only apparent when examining all the stars in the galaxy where discrete ‘streams’ with chemical properties distinct from the rest of the galaxy are seen. These arise from accretion of satellites that have lower [Fe/H] values and remain chemically distinct. Larger mergers may have a similar abundance to the primary galaxy but bring gas that can reignite a quiescent galaxy and accelerate the production of Fe in the short term.

## 5 SUMMARY

We present a new chemodynamical simulation code that produces feedback to account for long-lived stars and the elements that they produce. The more sophisticated SN feedback scheme improves the kinematic properties of the stellar fraction (this will be detailed in future work) and gives access to additional constraints on the subgrid physics. It is clear that the galactic CE for our $L_\star$ galaxy does not perfectly reproduce Milky Way observations; however, we believe it serves to demonstrate the validity of this approach. Future work using this code may merit the inclusion of cutting edge nucleosynthesis models (e.g. Doherty et al. 2010) and will make a comprehensive study of the influence of the parameters involved in the underlying CE model.

## ACKNOWLEDGMENTS

The authors thank the referee for their helpful comments. CGF acknowledges the support of the Science & Technology Facilities Council (ST/F007701/1). BKG acknowledges the support of the STFC (ST/F002432/1; ST/G003025/1), Monash University (the Kevin Westfold Distinguished Visitor Programme) and Saint Mary’s University. SC acknowledges support from the BINGO Project (ANR-08-BLAN-0316-01) and the CC-IN2P3 Computing Center (Lyon/Villeurbanne, France), a partnership between CNRS/IN2P3 and CEA/DSM/Irfu. DK acknowledges the support of the STFC (ST/H00260X/1). Computing resources were provided by the UK National Cosmology Supercomputer (COSMOS), the University of Central Lancashire’s HPC facility and the HPC resources of CINES under the allocation 2010-c2011046642 made by GENCI (Grand Equipement National de Calcul Intensif).

## REFERENCES

Agertz O. et al., 2007, MNRAS, 380, 963
Anders E., Grevesse N., 1989, Geochimica Cosmochimica Acta, 53, 197
Bensby T., Feltzing S., Lundström I., Ilyin I., 2005, A&A, 433, 185



Downloaded from http://mnrasl.oxfordjournals.org/ at Saint Mary's University on November 5, 2014

Carbon D. F., Barbuy B., Kraft R. P., Friel E. D., Suntzeff N. B., 1987, PASP, 99, 335
Carigi L., 1994, ApJ, 424, 181
Cayrel R. et al., 2004, A&A, 416, 1117
Chiappini C., Matteucci F., Gratton R., 1997, ApJ, 477, 765
Doherty C. L., Siess L., Lattanzio J. C., Gil-Pons P., 2010, MNRAS, 401, 1453
Dubois Y., Teyssier R., 2008, A&A, 477, 79
Edvardsson B., Andersen J., Gustafsson B., Lambert D. L., Nissen P. E., Tomkin J., 1993, A&AS, 102, 603
Gibson B. K., 1997, MNRAS, 290, 471
Gratton R. G., Carretta E., Claudi R., Lucatello S., Barbieri M., 2003, A&A, 404, 187
Hachisu I., Kato M., Nomoto K., 1999, ApJ, 522, 487
Iwamoto K., Brachwitz F., Nomoto K., Kishimoto N., Umeda H., Hix W. R., Thielemann F., 1999, ApJS, 125, 439
Kawata D., Gibson B. K., 2003, MNRAS, 340, 908
Kobayashi C., 2004, MNRAS, 347, 740
Kobayashi C., Tsujimoto T., Nomoto K., 2000, ApJ, 539, 26
Kodama T., Arimoto N., 1997, A&A, 320, 41
Kroupa P., 2001, MNRAS, 322, 231
Lia C., Portinari L., Carraro G., 2002, MNRAS, 330, 821
Mannucci F., Maoz D., Sharon K., Botticella M. T., Della Valle M., Gal-Yam A., Panagia N., 2008, MNRAS, 383, 1121
Martínez-Serrano F. J., Domínguez-Tenreiro R., Mollá M., 2008, in Bureau M., Athanassoula E., Barbuy B., eds, Proc. IAU Symp. 245, SPH Simulations of the Chemical Evolution of Bulges. Cambridge Univ. Press, Cambridge, p. 35
Matteucci F., Francois P., 1989, MNRAS, 239, 885
Oppenheimer B. D., Davé R., 2008, MNRAS, 387, 577
O'Shea B. W., Nagamine K., Springel V., Hernquist L., Norman M. L., 2005, ApJS, 160, 1
Pagel B. E. J., Patchett B. E., 1975, MNRAS, 172, 13
Pilkington K., Gibson B. K., Jones D. H., 2012, preprint (astro-ph/1203.1996)
Pilkington K. et al., 2012, A&A, 540, A56
Ramírez I., Allende Prieto C., Lambert D. L., 2007, A&A, 465, 271
Reddy B. E., Tomkin J., Lambert D. L., Allende Prieto C., 2003, MNRAS, 340, 304
Reddy B. E., Lambert D. L., Allende Prieto C., 2006, MNRAS, 367, 1329
Romeo A. D., Portinari L., Sommer-Larsen J., 2005, MNRAS, 361, 983
Sánchez-Blázquez P., Courty S., Gibson B. K., Brook C. B., 2009, MNRAS, 398, 591
Scannapieco C., Tissera P. B., White S. D. M., Springel V., 2005, MNRAS, 364, 552
Shen S., Wadsley J., Stinson G., 2010, MNRAS, 407, 1581
Talbot R. J., Jr, Arnett W. D., 1971, ApJ, 170, 409
Tasker E. J., Brunino R., Mitchell N. L., Michielsen D., Hopton S., Pearce F. R., Bryan G. L., Theuns T., 2008, MNRAS, 390, 1267
Teyssier R., 2002, A&A, 385, 337
Timmes F. X., Woosley S. E., Weaver T. A., 1995, ApJS, 98, 617
Tinsley B. M., 1980, Fundam. Cosmic Phys., 5, 287
Tornatore L., Borgani S., Matteucci F., Recchi S., Tozzi P., 2004, MNRAS, 349, L19
Valdarnini R., 2003, MNRAS, 339, 1117
van den Hoek L. B., Groenewegen M. A. T., 1997, A&AS, 123, 305
Wiersma R. P. C., Schaye J., Theuns T., Dalla Vecchia C., Tornatore L., 2009, MNRAS, 399, 574
Woosley S. E., Weaver T. A., 1995, ApJS, 101, 181

This paper has been typeset from a TEX/LATEX file prepared by the author.

Downloaded from http://mnrasl.oxfordjournals.org/ at Saint Mary's University on November 5, 2014

© 2012 The Authors, MNRAS **424,** L11–L15
Monthly Notices of the Royal Astronomical Society © 2012 RAS